

# The Variability of Paleoproductivity Proxies in Nearshore East Coast Peninsular Malaysia During Holocene

Hamad Maalim Sharif<sup>1,3</sup>, Fatin Izzati Minhat<sup>2</sup>, Kamaruzzaman Yunus<sup>4</sup>, Erick Naim<sup>5</sup>,  
Hasrizal Shaari<sup>1,2\*</sup>

<sup>1</sup>Institute of Oceanography and Environment, Universiti Malaysia Terengganu

<sup>2</sup>Faculty of Science and Marine Environment, Universiti Malaysia Terengganu  
21030, Kuala Nerus, Terengganu, Malaysia

<sup>3</sup>Zanzibar Fisheries and Marine Resources Research Institute  
P.O.BOX 2789, Zanzibar, Tanzania

<sup>4</sup>Department of Marine Science, Kulliyah of Science, International Islamic University Malaysia  
Bandar Indera Mahkota, 25200 Kuantan, Pahang, Malaysia

<sup>5</sup>Graduate School of Environmental Science, Hokkaido University  
Kita-10, Nishi-5, Kita-ku, Sapporo 060-0810 Japan  
Email: riz@umt.edu.my

## Abstract

The Holocene epoch was marked by significant climatic fluctuations that shaped marine productivity across tropical coasts. This study reconstructs Holocene paleoproductivity along the East Coast of Peninsular Malaysia, specifically Terengganu (TER16-GC13C) and Kelantan waters (KELC17) using core sediments. A multi-proxy approach was applied, analysing biogenic silica (BSi), total organic carbon (TOC), calcium carbonate ( $\text{CaCO}_3$ ), and elemental ratios ( $\text{Ca}/\text{Al}$ ,  $\text{Ca}/\text{Fe}$ ,  $\text{Ba}/\text{Al}$ ) to evaluate changes in productivity in response to sea-level and monsoonal variability. Results indicate distinct temporal patterns: the early Holocene showed elevated BSi and TOC linked to enhanced nutrient influx during rapid sea-level rise. While the mid-Holocene exhibited reduced carbonate deposition due to strong terrigenous input associated with the East Asian Summer Monsoon and the late Holocene was marked by increased  $\text{CaCO}_3$  deposition reflecting reduced riverine input and greater biogenic production during sea-level highstand decline. Elemental ratios corroborate these shifts, highlighting the dynamic interplay between terrigenous and marine sources. These findings demonstrate that sea-level change was a dominant driver of productivity variations, modulated by monsoonal strength. The strong correlation between terrigenous proxies and grain size underlines the role of hydrodynamics in sediment delivery. This study contributes an integrated Holocene paleoproductivity reconstruction for East Coast Peninsular Malaysia, providing a regional baseline that complements South China Sea records. The results enhance understanding of tropical shelf ecosystem sensitivity to climate variability, offering a reference framework for assessing future climate change impacts on coastal productivity.

**Keywords:** South China Sea, Sunda shelf, Tropical, Sea level, Biogenic Silica, Calcium Carbonate

## Introduction

The Holocene epoch approximately 11,700 years, signifies a crucial phase in Earth's history marked by substantial climatic and environmental transformations (Smith *et al.*, 2011). This era has seen the emergence of contemporary ecosystems, positioning it as a critical area for comprehending historical climate variability and its consequences for future environmental circumstances. The examination of paleoproductivity, denoting the past biological productivity in marine ecosystems, yields significant insights into the interplay between climate, oceanographic conditions, and ecosystem dynamics during this epoch (Zhou *et al.*, 2023).

On the East Coast of Peninsular Malaysia, the interaction of monsoonal impacts and coastal oceanographic processes has significantly impacted the coastal ecosystems. The reconstruction of paleoproductivity in this region during the Holocene provides a chance to examine how variations in environmental conditions, including sea level changes and nutrient availability, have influenced the area's biological productivity. These reconstructions are crucial for comprehending the region's reaction to historical climate fluctuations and guiding future environmental management approaches.

Biogenic silica (BSi) is a principal biogenic constituent in marine sediments and serves as a

suitable proxy for productivity. This opal derives from the frustules of diatoms or the skeletal remains of radiolarians and sponges. Diatoms constitute almost 40% of the world's primary output, indicating a significant interplay between the ocean's silica and carbon cycles (Isla, 2016; B-Béres *et al.*, 2023). The accumulation of BSi in sediments indicates the overall pattern of primary production in the underlying seas (Liu *et al.*, 2021) and can, therefore, serve as a proxy for paleoproductivity research (Song, 2010; Xu *et al.*, 2019).

Calcium carbonate ( $\text{CaCO}_3$ ) constitutes the principal element of the skeletal structures of marine creatures such as corals, molluscs, and foraminifera (Morse *et al.*, 2007). Grassle (1973) asserted that carbonate particles are effectively retained during the transfer of flux to the seabed. Thus, nearly all carbonate in the upper ocean is derived by calcifying marine creatures that contribute to the carbonate flux to the sediment (Geyman *et al.*, 2022).

The total organic carbon (TOC) may serve as a proxy for fluvial discharge, with its variability potentially indicating alterations in terrigenous input and fluvial discharge. Higher TOC levels are associated with increased fluvial discharge volumes and vice versa (Huang *et al.*, 2020; Xu *et al.*, 2022). Elevated TOC levels may be attributed to an increased influx of terrestrial material from a broader region and deeper organic-rich regolith within the rivers (Huang *et al.*, 2020; Xu *et al.*, 2022).

This study compares BSi, TOC,  $\text{CaCO}_3$ , and selected geochemical elements in sediment cores from the nearshore regions of the East Coast of Peninsular Malaysia to provide a thorough reconstruction of Holocene paleoproductivity. The study aims to evaluate the comparative efficacy of these proxies in reflecting past productivity indicators and to discern the environmental factors that have impacted regional productivity. Moreover, the findings help establish an initial regional dataset, enhancing the investigation of global climatic and environmental processes throughout this period.

## Materials and Methods

The study was conducted in the coastal waters of Terengganu, located off the northeastern margin of Peninsular Malaysia (Figure 1). This region lies at the interface between the shallow, semi-enclosed South China Sea and the deeper Gulf of Thailand. The study area is situated on a broad continental shelf, with average water depths generally less than 100 m (Azmi *et al.*, 2020). The area experiences a tropical monsoonal climate, influenced by two distinct seasonal wind systems: the northeast monsoon (November to March) and the southwest monsoon (April to August) (Kok *et al.*, 2022). During the northeast monsoon, wave heights can reach up to 4 m, whereas wave activity during the southwest monsoon is relatively calm, with maximum heights typically below 1 m (Nasir *et al.*, 2022).

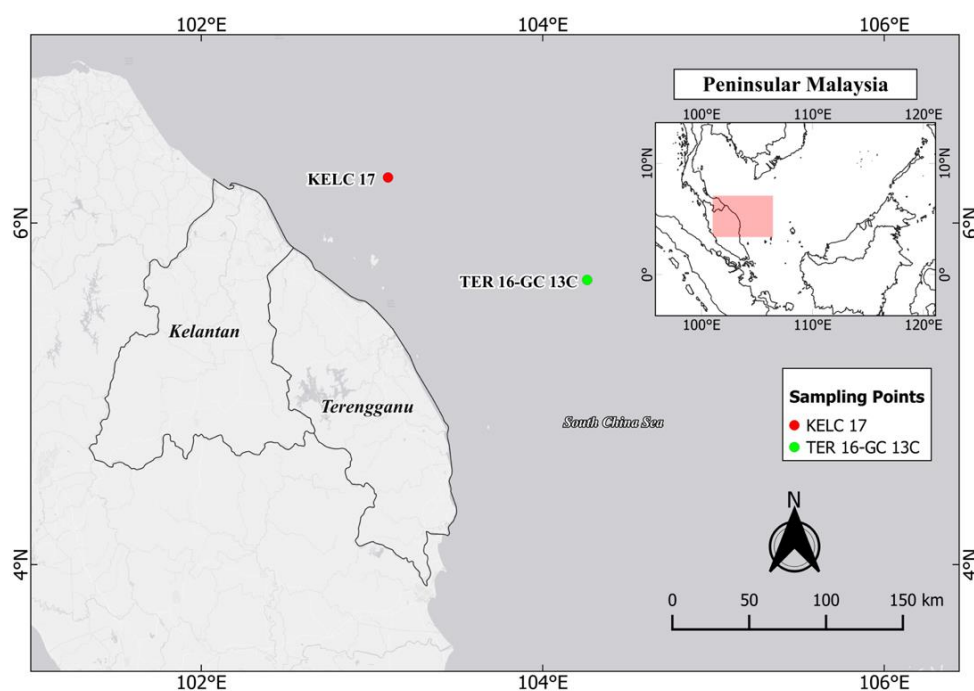


**Figure 1.** Map showing the sampling locations for TER16-GC13C and KELC17 in the nearshore area of East Coast Peninsular Malaysia

Sea surface temperatures in the region range from 30 to 32 °C, while salinity values generally vary between 31.5 and 32.1 parts per thousand (Kok *et al.*, 2022). The coastal zone receives substantial terrigenous input, primarily from the Terengganu River and several smaller tributaries that discharge directly into the South China Sea, contributing to the dynamic sedimentary and hydrological characteristics of the area.

### Sample collection and preservation

Using a gravity corer, the marine core sediment of TER16-GC13C and KELC17 was recovered in 2016 aboard the RV Discovery at 70nm (5°39.993' N, 104°15.632' E, 73 m water depth) and 51 nm (6°15.933'N, 103°5.634' E, 54 m water depth) from the coastlines of Kuala Terengganu and Kelantan (Figure 1) (Naim *et al.*, 2019). After being collected, the sediment cores were returned to the laboratory for subsampling. To avoid potential contamination, the subsampled sediments were freeze-dried for three days and then stored in cleaned and labelled containers after being frozen at 4 °C for 24 hours. Samples for the BSi, TOC, and CaCO<sub>3</sub> analyses were powdered and mixed using an agate mortar before being sieved through a 150 µm mesh sieve. The sediments for particle size analysis were stored in cleaned containers without being powdered.

### Biogenic Silica analysis

Biogenic silica (BSi) was extracted from samples through a modified sequential alkaline extraction Demaster (2000) and Mortlock and Froelich (1989). Approximately 40 mg of dried sediment samples were crushed and weighed in a 50 ml flat-bottomed polypropylene digestion vessel. 40ml of sodium carbonate (1%) was added and placed in a heating block at 85 °C. Subsampling was performed at 3, 4, and 5 hours of heating. The digestion vessels were cooled down in a room-temperature water bath for about 5 minutes to stop further BSi extraction and reduce pipetting errors due to thermal expansion. 1 ml was removed from the extraction solution and stored in 50 ml polypropylene centrifuge tubes and held in the chiller until further analysis. Samples were left to stand at room temperature for one hour before spectrophotometric analysis using the Molybdenum blue method modified from (Shapiro and Brannock, 1962). 1.5 ml ammonium molybdate was added into the extractant, shaken, and left to stand for 10 minutes. Then, 1.25 ml of 25% sulphuric acid (H<sub>2</sub>SO<sub>4</sub>) and 1 ml reducing solution were added to the extractant. The addition of 0.021 N HCl was used to neutralize the solution. The extractant was left to stand for 30 minutes before detection using a Shimadzu UV-1800 UV-VIS spectrophotometer at 640 nm. The concentration of

BSi was obtained from the silica standard curve constructed in the range of 0-5 ppm. The concentration of BSi was calculated based on the proposed calculation by Demaster (2000):

$$\text{Concentration of SiO}_2 = \text{Absorbance}/K \quad (1)$$

Where K is the slope of the standard curve

$$\text{SiO}_2 (\%) = [\text{Concentration of SiO}_2 (\text{ppm}) / \text{Weight of samples (g)}] / 100000 \quad (2)$$

### Total carbon analysis

Sediment samples were analysed for total carbon (TC) and inorganic carbon (IC) content via a Shimadzu TOC Analyser paired with a Shimadzu Solid Sample Module SSM-5000A at the Centre of Research and Field Service, Universiti Malaysia Terengganu (UMT). The ceramic sample boats and glass wool utilised in the analysis were incinerated at 400 °C for 4 hours. For TC analysis, 10 mg of the homogenised material was incinerated at 900 °C. For IC analysis, 10 mg of homogenised material was subjected to digestion with 60% phosphoric acid at 200 °C. For quality control, standard research materials (glucose and sodium carbonate for TC and IC analysis) were examined throughout each session, achieving 100% recovery. The TOC values were derived by deducting the IC value from the TC value. The values of CaCO<sub>3</sub> were derived by multiplying the IC values by 8.33, which represents the ratio of the molecular mass of CaCO<sub>3</sub> to that of carbon (100/12), under the premise that all inorganic carbon is in the form of pure calcite.

### Grain size analysis

Grain size analysis was performed following the procedure in Kamaruzzaman *et al.* (2008) with some modifications. About 2 g of dried sample was weighed in clean plastic containers. 10 drops of undiluted hydrogen peroxide were added to the samples, followed by 5 mL of 20% sodium hexametaphosphate. Distilled water was then added to the volume, and the samples were left to stand for 24 hours. Next, the samples were analysed using a Malvern Mastersizer 2000™ laser diffraction particle size analyser.

### Elemental analysis

The samples were digested and analysed using the modified methods of Kamaruzzaman *et al.*, (2008). Approximately 0.25 g of powdered sediment samples were placed in a Teflon vessel and digested in mixed acid of 1 mL perchloric acid (HClO<sub>4</sub>), 1 mL hydrogen peroxide (H<sub>2</sub>O<sub>2</sub>), and 6 mL nitric acid (HNO<sub>3</sub>) in a microwave digester. The digestion process was

set at the temperature of 100 °C for 7 hours. After cooling, the clear digested sample was transferred into a 50 mL centrifuge tube and added with milli-Q water to 50 mL. After an appropriate dilution, the samples were analysed for elemental composition by a Perkin Elmer ELAN 9000 Inductively Coupled Plasma Mass Spectrometer (ICP-MS) in the Institute of Oceanography and Environment (INOS), Universiti Malaysia Terengganu (UMT). The accuracy of the analytical procedure was examined by analysing standard research material (SRM) NBS1646a estuarine sediment in duplicate and blank as control. The recovery test of four elements in the certified value of NBS1646a was 82.67% for iron (Fe), 86.48% for barium (Ba), 95.78 for aluminium (Al), and 98.26% for calcium (Ca).

## Result and Discussion

### Distribution profile of marine proxies

The composition of BSi in TER16-GC13C varied between 0.01 and 1.83%, with slightly higher values in the late Holocene ( $0.77 \pm 0.45\%$ ) and lower composition in the mid-Holocene ( $0.49 \pm 0.38\%$ ) (Figure 2). The BSi content in KELC17 averaged

$0.50 \pm 0.27\%$ , varying between 0.06 and 1.3%, but relatively stable concentrations across the entire core (Figure 3). Biogenic silica, primarily consisting of remains from diatoms, radiolarians, and sponge spicules, constitutes a crucial element of marine sediments present at all depths, latitudes, and climatic zones in the world's oceans (Sun *et al.*, 2020). Thus, variations in BSi content in sedimentary records are frequently used for paleoenvironmental reconstruction (Ragueneau *et al.*, 2000).

The higher BSi levels observed in the early Holocene might be due to rising sea levels, which inundated continental shelves, enhancing nutrient influx from river systems and estuaries and thus promoting diatom productivity in the region (Douglas *et al.*, 2007). In the mid-Holocene, sea levels stabilised, resulting in a higher BSi deposition. The low BSi levels in the late Holocene were related to the decreased nutrient availability in surface waters (Zhang *et al.*, 2015). In general, the BSi displays a pattern similar to TOC, increasing during the early Holocene coinciding with rising sea levels, while  $\text{CaCO}_3$  shows a decreasing pattern. In the late Holocene, an inverse pattern is noted, with  $\text{CaCO}_3$  increasing while BSi and TOC concentrations declined (Hahn *et al.*, 2016; Zhao *et al.*, 2017).

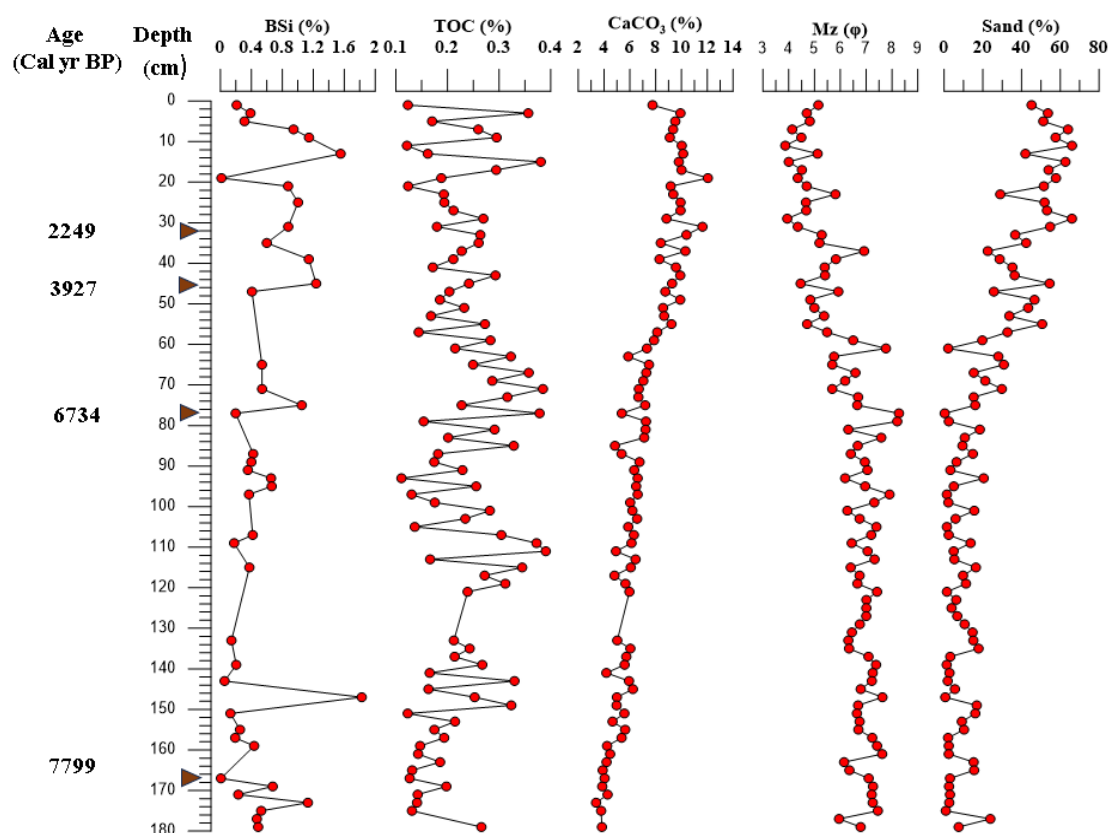


**Figure 2.** The distribution profile of BSi (This study), TOC,  $\text{CaCO}_3$  (Naim *et al.*, 2019), Mz and Sand (This study) in Core TER16-GC13C

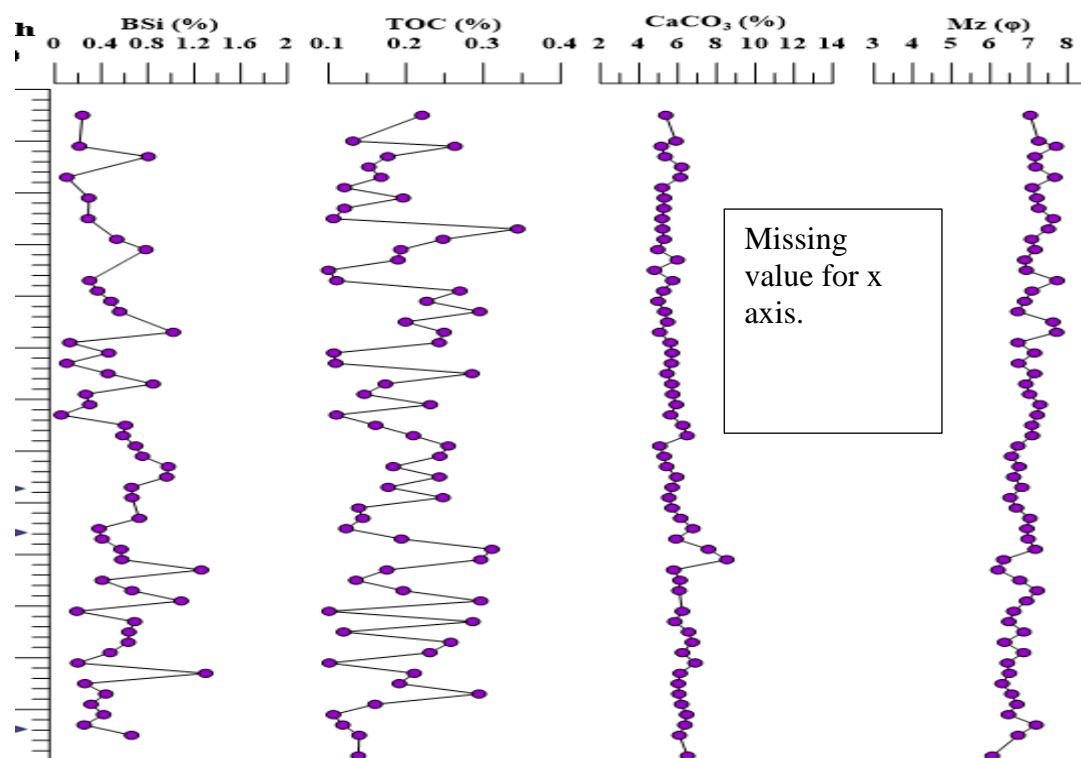


**Figure 3.** The distribution profile of BSi, TOC,  $\text{CaCO}_3$ , Mz and Sand in Core KELC17

In this study, the variations in TOC concentrations indicate the proportion of fluvial discharge. TOC content in TER16-GC13C and KELC17 was flat, with approximately the same content in both cores. In TER16-GC13C, TOC content ranged from 0.11 to 0.39% and was nearly constant throughout the core from the late to mid-Holocene (Figure 2), while in the core KELC17, it varied from 0.10 to 0.34%, with an average concentration of about  $0.19 \pm 0.07\%$  (Figure 4). The enhanced TOC value could also be associated with an increase in river runoff, which supplied large amounts of TOC into the shelf area, particularly during NE monsoon (Shaari *et al.*, 2009; Yun *et al.*, 2015). On the other hand, the lower TOC abundance from the mid-to late-Holocene might result from declining the terrestrial influx.

$\text{CaCO}_3$  content in TER16-GC13C exhibited higher composition in the late Holocene ( $9.63 \pm 0.94\%$ ) and a lower range in the mid-Holocene ( $5.88 \pm 1.30\%$ ) but decreasing slightly to 3.38 % (Figure 2). KELC17 showed that  $\text{CaCO}_3$  content varied from 4.80% to 8.53%, with an average value of  $5.85 \pm 0.68\%$ . The variation in  $\text{CaCO}_3$  concentration was almost constant throughout the core, showing a decreasing trend from the late to early Holocene (Figure 3). The carbonate deposition is affected by several factors, including the rate of sea surface carbonate production, the dilution of terrigenous

materials, and the preservation conditions of bottom water (Huang *et al.*, 2015). The lower  $\text{CaCO}_3$  concentration, which corresponds to the high terrigenous input in the early to mid-Holocene, was suggested to be due to the dilution effect caused by the higher terrigenous influx (Tribovillard *et al.*, 2006; Huang *et al.*, 2015). This period is also considered an extremely weathering period in the SCS attributed to the strong EASM (Yang *et al.*, 2008; Hu *et al.*, 2012; Huang *et al.*, 2015). On the contrary, the increase in  $\text{CaCO}_3$  in the late Holocene suggests that the sea level rise reduced the total terrigenous flux and the warm climate that promoted calcareous productivity (Li *et al.*, 2018; Naim *et al.*, 2019). The carbonate content variations are attributed to changes in terrestrial sediment input in response to sea level fluctuations. Tetapi senario ini berbeza bagi  $\text{CaCO}_3$  core KELC17.

Aluminium content in TER16-GC13C sediment cores increased with depth (Figure 4). The average composition of Al in TER16-GC13C was  $9.41 \pm 2.82\%$ , increasing from  $5.83 \pm 1.04\%$  in the late Holocene to  $10.78 \pm 1.93\%$  in the mid-Holocene. The average Al concentration in the KELC17 sediment core was  $1.99 \pm 0.29\%$ , showing a slightly increasing pattern down the core (Figure 5). The average concentration of Al was higher in TER16-GC13C ( $9.41 \pm 2.82\%$ ) compared to KELC17 ( $1.99 \pm 0.29\%$ ). Iron contents in all cores

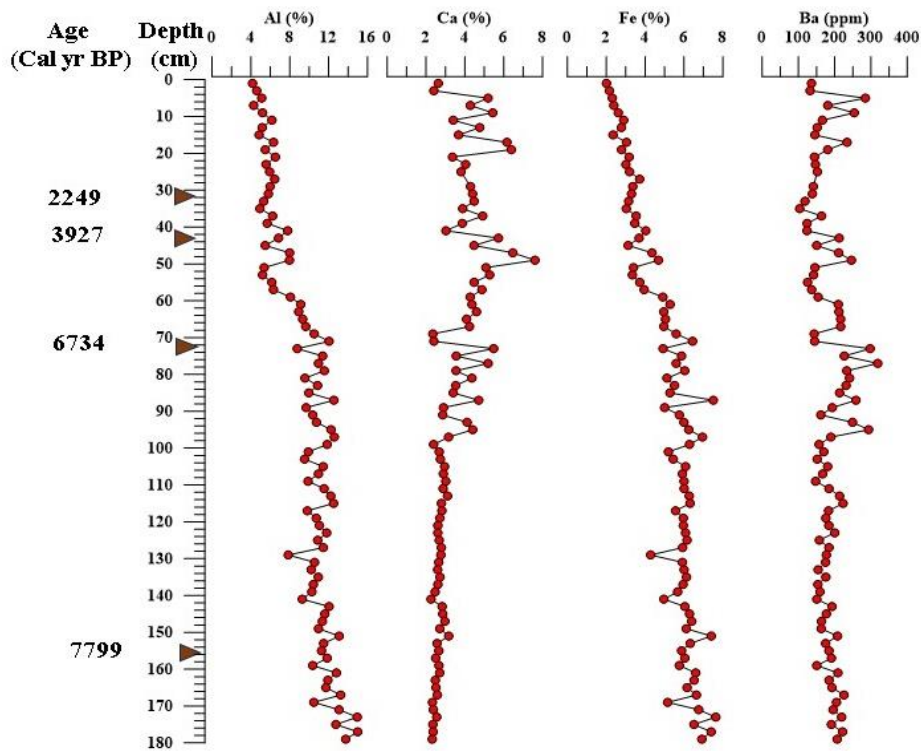


Figure 4. Variations in the concentration of selected elements of Al, Ca, Fe (Sharif *et al.*, 2024) and Ba in Core TER16-GC13C

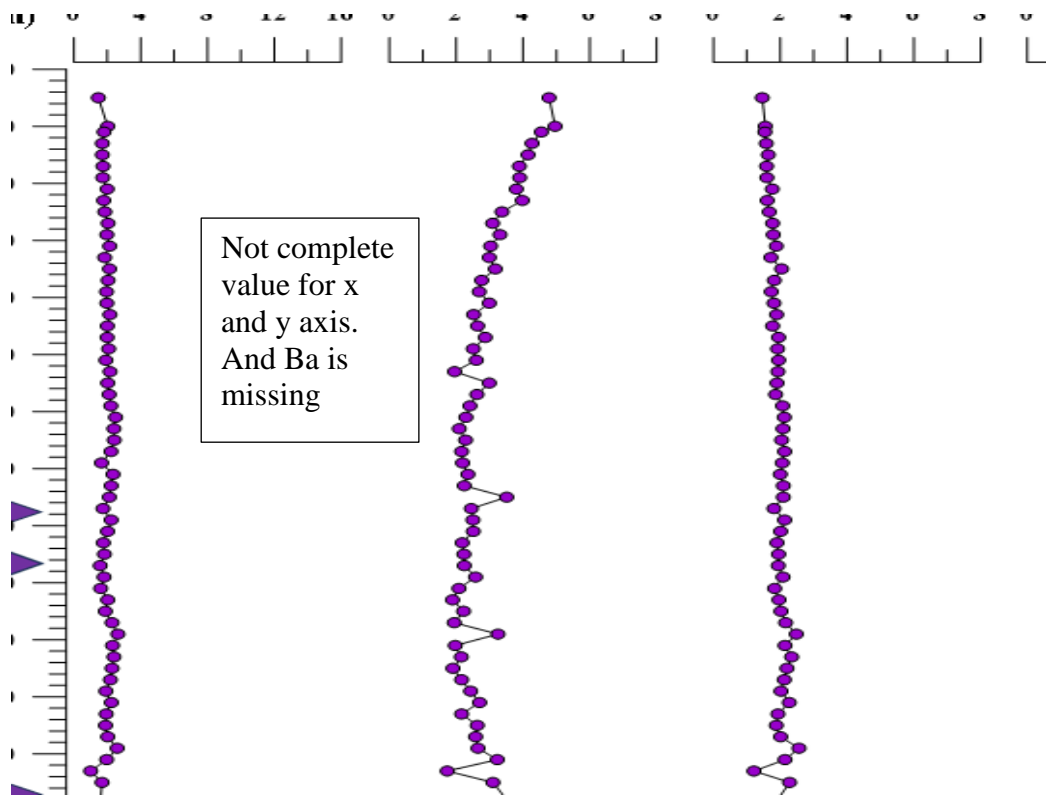


Figure 5. Variations in concentration of Selected elements of Al, Ca, Fe and Ba in Core KELC17 during Holocene



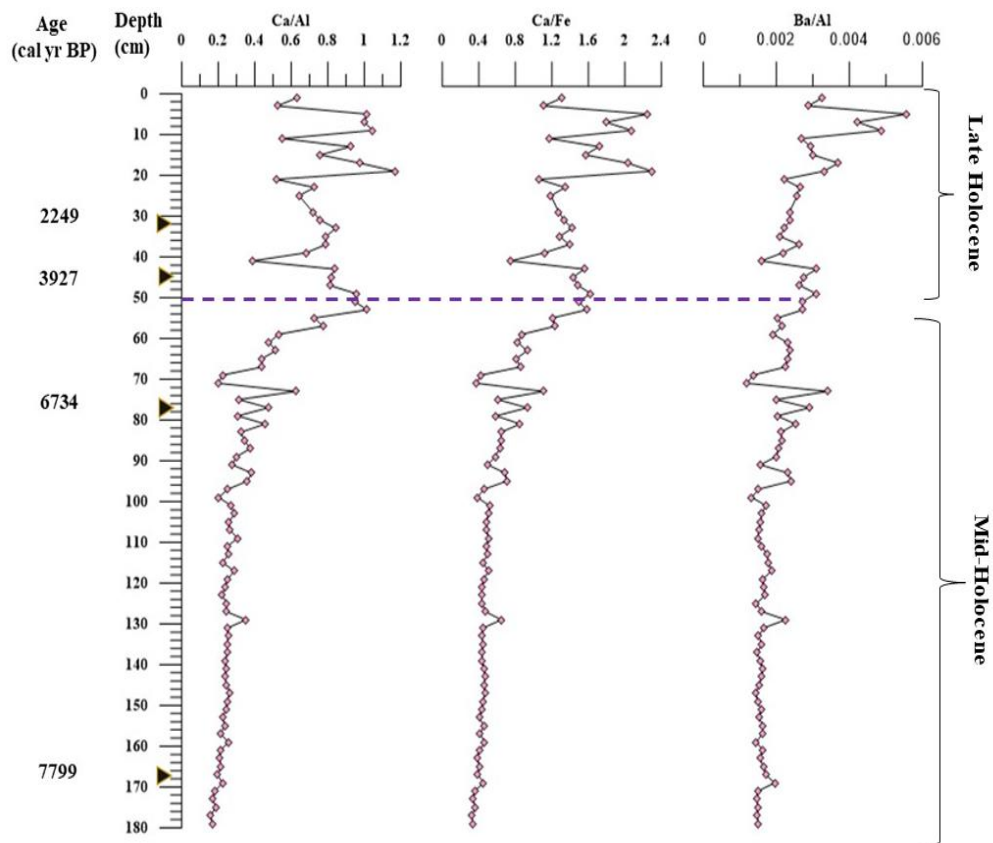


Figure 6. The ratio of Ca/Al and Ca/Fe, (Sharif et al., 2024), and Ba/Al in core TER16-GC13C During the Holocene

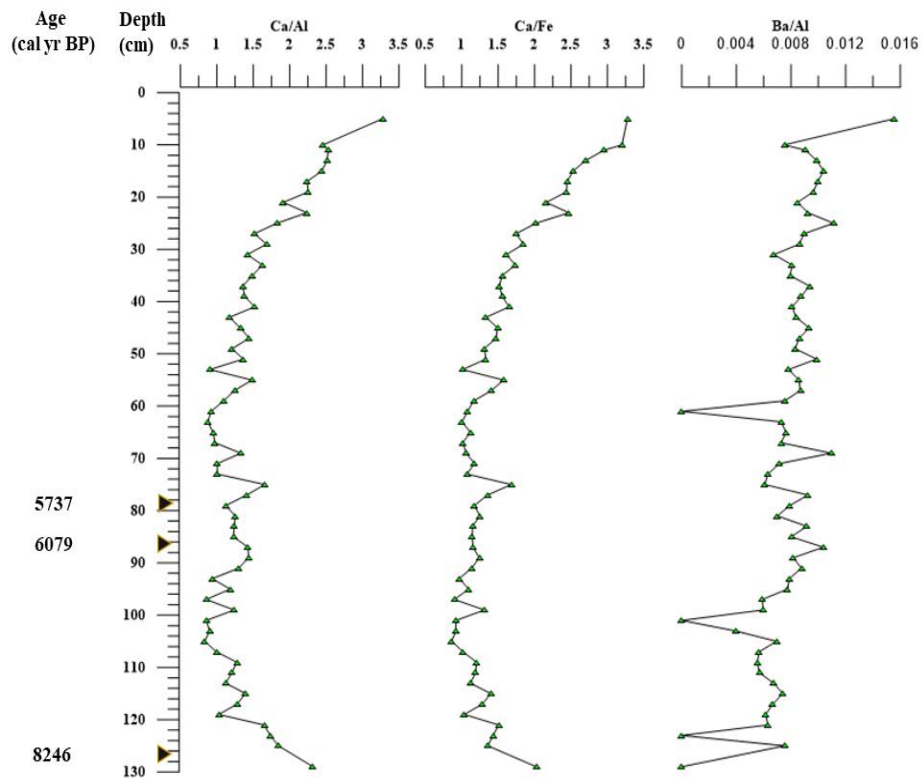


Figure 7. The ratio of Ca/Al, Ca/Fe, and Ba/Al in core KELC17 During Holocene

investigated (TER16-GC13C and KELC 17) showed a similar downward increasing pattern. However, apparent changes were uncovered in TER16-GC13C while only slightly increasing downward in KELC 17. In TER16-GC13C, the Fe abundance averaged  $5.07 \pm 1.46$  %, fluctuating from  $3.13 \pm 0.66$  % in the late Holocene to its highest value of  $5.82 \pm 0.88$  % in the mid-Holocene. The average Fe composition in KELC17 was  $1.93 \pm 0.24$  %, marginally increasing down the core. The composition of Fe was highest in TER16-GC13C ( $5.07 \pm 1.46$  %), followed by KELC17 ( $1.93 \pm 0.24$  %).

Variations of Ca abundances in TER16-GC13C and KELC17 decreased with depth, opposing the trend of other elements. Following the same pattern, the proportion of Ca in TER16-GC13C had a median of  $3.54 \pm 1.16$  %, changing from  $4.53 \pm 1.28$  % in the late Holocene and declining to  $3.18 \pm 0.88$  % in the mid-Holocene. The highest Ca content was displayed in TER16-GC13C ( $3.54 \pm 1.16$  %) than KELC17 ( $2.80 \pm 0.76$  %). Ba in TER16-GC13C, the Ba concentration averaged 185.02 ppm, increasing from  $168.28 \pm 47.78$  ppm in the late Holocene and rose to  $191.20 \pm 38.96$  ppm in the mid-Holocene. The Ba abundance in KELC17 had a mean of  $159.32 \pm 23.70$  ppm, which varied slowly downward. The maximum composition was recorded in TER16-GC13C as  $185.02 \pm 42.49$  ppm, followed by KELC17 with  $159.32 \pm 23.70$  ppm.

Elemental ratios of Ca/Al, Ca/Fe, and Ba/Al serve as good proxies for reconstructing past environmental conditions (Messa-Fenández *et al.*, 2022). The Ca/Al ratio in TER16-GC13C and KELC17 sediment cores fluctuated from 0.16 to 1.17 and 0.83 to 3.27, with average values of 0.45 and 1.47, respectively (Figure 6). The ratio of Ca to Al in TER16-GC13C sediment cores demonstrated a decreasing pattern down the core, displaying higher values during the late Holocene and the lowest ratio in the early Holocene. In the TER16-GC 13C sediment core, the mean Ca/Al declined from  $0.79 \pm 0.19$  in the late Holocene to  $0.32 \pm 0.15$  in the mid-Holocene. The KELC17 sediment core represents the mid-Holocene era only, displaying an average Ca/Al of  $1.47 \pm 0.51$ .

The Ca/Fe ratio in TER16-GC13C sediment cores showed higher ratios in the late Holocene and declined to the lowest ratios in the early Holocene. The ratio varied from 0.32 to 2.30 and 0.86 to 3.27 in TER16-GC13C and KELC17 sediment cores, respectively. The average Ca/Fe in TER16-GC13C declined from  $1.49 \pm 0.38$  in the late Holocene to  $0.58 \pm 0.24$  in the mid-Holocene. In the KELC17 sediment core (Figure 7), the mean Ca/Fe was  $1.52 \pm 0.58$ . The Ba/Al ratio demonstrated a similar pattern as Ca/Al and Ca/Fe in TER16-GC13C sediment cores, varying from 0.0012 to 0.0056 and

0.0039 to 0.0156 in cores TER 16-GC 13C and KELC17, respectively. The average Ba/Al in TER16-GC13C was recorded as  $0.0030 \pm 0.0009$  in the late Holocene and declined to  $0.0018 \pm 0.0004$ . The Ba/Al demonstrated a similar pattern as Ca/Al and Ca/Fe in KELC 17, decreasing slightly in the mid-Holocene. The average Ba/Al in the KELC 17 was  $0.0082 \pm 0.0018$ .

In the early to mid-Holocene, low ratios of Ca/Al, Ca/Fe, and Ba/Al suggest an increased influx of land-derived materials that diluted marine-origin materials. In contrast, higher ratios in the late Holocene indicate an increased prevalence of biogenic materials, reducing the influence of land-derived materials (Jaccard *et al.*, 2010; Liu *et al.*, 2017). The concentrations of terrigenous elements were higher in the early Holocene. However, they slightly increased in the mid-Holocene, suggesting a greater volume of terrigenous material discharge during this period. This occurred at the beginning of the mid-Holocene when the rate of sea level dropped and reached zero at approximately 5000 cal yr BP in the ECPM (Twarog *et al.*, 2021; Zhang *et al.*, 2021). Therefore, the increased Ca/Al, Ca/Fe, and Ba/Al ratios during the late Holocene resulted from decreased terrigenous input, while the low ratios in the early to mid-Holocene were due to the increased terrigenous influx caused by the stable sea level (Jiwarungrueangkul *et al.*, 2019; Wang *et al.*, 2020).

### Statistical analysis

The results of the Pearson correlation analysis for sediment cores from Terengganu and Kelantan reveal significant differences in the relationships between major geochemical components, reflecting distinct depositional environments and sedimentary processes along the East Coast of Peninsular Malaysia (Table 1 and Table 2).

In the Terengganu (TER16-GC13C), Al and Fe exhibit an exceptionally strong positive correlation ( $r = 0.979$ ,  $P < 0.01$ ), suggesting a common source for these elements, likely driven by terrigenous input from riverine discharge or coastal erosion (Table 1). This finding aligns with previous studies indicating that Fe and Al often co-vary in detrital sediments, reflecting their association with clay minerals and terrestrial material (Gingele *et al.*, 2004). In contrast, the Kelantan core (KELC17) shows a weaker but still significant correlation between Al and Fe ( $r = 0.728$ ,  $P < 0.01$ ) (Table 2), suggesting that while terrigenous input is still important, there may be a greater influence of other sedimentary components such biogenic material that dilute this relationship.

Calcium and Al exhibit a moderate negative correlation in the Terengganu core ( $r = -0.510$ ,  $P < 0.01$ ), indicating that carbonate and siliciclastic materials are deposited under contrasting conditions



**Table 1.** Pearson's Correlation Matrix for Selected Geochemical Elements, TOC, CaCO<sub>3</sub> and BSi in Core TER16-GC13C

	Al	Ca	Fe	Ba	TOC	CaCO <sub>3</sub>	BSi
Al	1						
Ca	-0.510**	1					
Fe	0.979**	-0.483**	1				
Ba	0.387**	0.302**	0.323**	1			
TOC	-0.086	0.089	-0.080	0.045	1		
CaCO <sub>3</sub>	-0.852**	0.583**	-0.848**	-0.237*	0.052	1	
BSi	-0.287	0.194	-0.270	-0.162	-0.040	0.263	1

\*\* Correlation is significant at the 0.01 level (2-tailed); \* Correlation is significant at the 0.05 level (2-tailed).

**Table 2.** Pearson's Correlation Matrix for Selected Geochemical Elements, TOC, CaCO<sub>3</sub> and BSi in Core KELC17

	Al	Ca	Fe	Ba	TOC	CaCO <sub>3</sub>	BSi
Al	1						
Ca	-0.276*	1					
Fe	0.728**	-0.499**	1				
Ba	-0.178	0.292*	-0.490**	1			
TOC	0.112	-0.022	0.091	-0.097	1		
CaCO <sub>3</sub>	-0.147	-0.309*	0.209	-0.408**	0.056	1	
BSi	0.099	-0.121	0.246	-0.189	0.340*	0.012	1

\*\* Correlation is significant at the 0.01 level (2-tailed); \* Correlation is significant at the 0.05 level (2-tailed).

or from different sources. This inverse relationship is further highlighted by the robust negative correlation between CaCO<sub>3</sub> and Al ( $r = -0.852$ ,  $P < 0.01$ ), suggesting that carbonate deposition, likely driven by biogenic activity, occurs during periods of reduced terrigenous input. This pattern is consistent with environments where coral reef or carbonate platform development dominates sedimentation (Perry *et al.*, 2012). In the Kelantan core, the correlation between Ca and Al is weaker ( $r = -0.276$ ,  $P < 0.05$ ). At the same time, the relationship between CaCO<sub>3</sub> and Al is minimal ( $r = -0.147$ ,  $P > 0.05$ ), indicating a more mixed depositional regime with less pronounced carbonate dominance.

This suggests deposition in relatively low-energy environments characterised by reduced current velocities, facilitating the settling of finer particles and organic matter (Liu *et al.*, 2022; Xia *et al.*, 2022). The observed negative correlation between TOC and CaCO<sub>3</sub> indicates that enhanced organic carbon content periods are related to reduced carbonate content and vice versa (Wang *et al.*, 2020). The correlation patterns observed highlight significant regional differences in sediment deposition along the East Coast of Peninsular Malaysia. Terengganu sediments are characterised by strong carbonate dominance and clear separation from terrigenous input, reflecting robust refill and biogenic processes. In contrast, Kelantan sediments

show more mixed depositional signatures, with less pronounced carbonate influence and greater variability in detrital contributions. These differences likely reflect variations in the proximity of the study site to the coastline, hydrodynamic conditions, and riverine discharge.

#### **Paleoenvironmental changes during holocene**

Our findings indicate that sea-level fluctuations are likely a primary factor influencing sedimentary archives and their reactions to environmental changes during the Holocene. The sedimentary records indicated notable fluctuations during the Holocene, as demonstrated by changes in the studied proxies. Sea level significantly influences the transport and deposition of terrigenous sediments in coastal habitats, supporting the conclusions of Jiwaringrueangkul *et al.* (2019). Mann *et al.* (2019) indicated that the sea level in the Malay-Thai Peninsula increased from -33 m mean sea level (msl) roughly 10,500 cal yr BP to its present level around 7000 cal yr BP. The mid-Holocene highstand occurred between 6000 and 4000 cal yr BP, with sea levels reaching an estimated elevation of 2 to 4 m above MSL.

Tam *et al.* (2018) reported a significant increase in sea levels along the ECPM, from  $-35 \pm 4.3$  m at 10,500 cal yr BP to  $-14.2 \pm 1.6$  m at 9000 cal yr

BP, with a swift rise rate of  $15.8 \pm 3.9$  mm yr<sup>-1</sup>. From 9000 to 5000 cal years BP, the rate of relative sea-level rise diminished, ultimately stabilising at a highstand of roughly  $3.3 \pm 0.2$  m. Thereafter, sea levels commenced a decrease, attaining  $-0.6 \pm 0.1$  m by 800 cal yr BP. These observations strongly correspond with our findings and those documented by Mann *et al.* (2019). The aforementioned environmental conditions have profoundly impacted the sedimentary patterns in the tropical seas of the ECPM. Our research focused on the principal environmental alterations during three specific phases of the early, mid, and late Holocene.

During the Early Holocene, the sea level rose rapidly, causing an increase in the distance between the location of core TER16-GC13C and the Terengganu River mouth. Therefore, the decrease in sediment discharge and consequent reduction pattern of terrigenous input can be attributed to changes in sea level. Meanwhile, the records from the TER16-GC13C sediment core exhibited an increasing trend of terrigenous input, as inferred by the high abundances of TOC in this period. This happened because the rising sea level had opposite effects on sedimentation. The sea level rise led to an increase in distance between the shoreline and the TER16-GC13C, negatively affecting the fluvial discharge. This, in turn, reduced the influx of terrigenous material. The longer transport distance from the Terengganu River mouth due to abrupt sea level rise in this period promoted the deposition of fine-grained sediments (6.37  $\phi$ ). However, compared to the mid- and late-Holocene, this period displayed slightly coarser sediment texture as inferred by the negative correlation with TOC (Table 1).

Mid-Holocene was recovered in both TER16-GC13C and KELC17 cores. At the beginning of the mid-Holocene, the rate of sea level rise slowed down and reduced to zero at about 5000 cal yr BP in the ECPM (Tam *et al.*, 2018; Zhang *et al.*, 2021). Consequently, the rise in sea level remained stable and had little impact on terrigenous input while the East Asian Summer Monsoon (EASM) strengthened. Besides, in the TER16-GC13C sediment core, the relatively high compositions of terrigenous elements (Al and Fe) and reduced Ca and CaCO<sub>3</sub> contents. During this period, a high influx of terrigenous material diluted biogenic matter, causing low values of Ca and CaCO<sub>3</sub> (Tribovillard *et al.*, 2006; Huang *et al.*, 2015).

The sediment grain size increased since the Mz and TOC were found to be strongly negatively correlated. The terrigenous elements (Al and Fe) strongly correlate with mean grain size, indicating that these elements are concentrated mainly in finer-grained sediments. Therefore, grain size greatly

influences the deposition of terrigenous elements. In the KELC17 core, the concentrations of terrigenous elements were almost constant, possibly due to the single source of sediment supply, the Kelantan River to Kelantan delta and then to the KELC17. The late Holocene interval represents the uppermost parts of core TER16-GC13C and KELC17. This period is marked by a decrease in sea levels, leading to diminished river flow, as seen by the low TOC percentage. Elevated levels of Ca and CaCO<sub>3</sub> may be associated with a significant influx of biogenic material during the late Holocene, which diminished the terrigenous components (Huang *et al.*, 2015). The decline in terrigenous composition concluded approximately 2000 cal years BP.

## Conclusions

The study provides an integrated Holocene paleoproductivity reconstruction for the East Coast of Peninsular Malaysia, based on multi-proxy analysis of sediment cores from Terengganu (TER16-GC13C) and Kelantan (KELC17) waters. The results show that productivity patterns were strongly influenced by sea-level fluctuations and monsoonal variability. During the early Holocene, rapid sea-level rise enhanced nutrient influx and diatom productivity, reflected in elevated BSi and TOC. The mid-Holocene, characterised by a stabilised sea level and intensified East Asian Summer Monsoon, saw greater terrigenous input diluting carbonate production. In the late Holocene, falling sea level reduced riverine input, favouring carbonate deposition from biogenic sources. Elemental ratios (Ca/Al, Ca/Fe, Ba/Al) confirm alternating dominance of terrigenous and marine contributions through time, while correlations with grain size underline the hydrodynamic control on sediment deposition. These findings demonstrate that local productivity was modulated by regional sea-level dynamics, monsoonal strength, and sediment delivery processes. The results provide essential context for interpreting the potential impacts of climate change on tropical coastal ecosystems.

## Acknowledgments

This work was supported by the Ministry of Higher Education Malaysia (MOHE) through the Fundamental Research Grant Scheme (grant number FRGS/1/2018/WAB09/UMT/02/3).

## References

- Azmi, N., Minhat, F.I., Hasan, S.S., Rahman Abdul Manaf, O.A., Abdul A'ziz, A.N., Wan Saelan, W.N., Shaari, H., Aziz, A.A. & Suratman, S., 2020. Distribution of benthic foraminifera off Kelantan, Peninsular Malaysia, South China Sea. *J. Foraminiferal Res.*, 50(1): 89-96.

- B-Béres, V., Stenger-Kovács, C., Buczkó, K., Padisák, J., Selmečzy, G.B., Lengyel, E. & Tapolczai, K., 2023. Ecosystem services provided by freshwater and marine diatoms. *Hydrobiologia*, 850(12): 2707-2733.
- Demaster, D.J. 2000. Measuring biogenic silica in marine sediments. *Mar. Chem.*, 68(3): 363–367. [https://doi.org/10.1016/S0304-4203\(99\)00079-1](https://doi.org/10.1016/S0304-4203(99)00079-1).
- Douglas R, Gonzalez-yajimovich O., Ledesma-vazquez J. & Staines-urias F. 2007. Climate forcing, primary production and the distribution of Holocene biogenic sediments in the Gulf of California. *Quaternary Sci. Rev.*, 26: 115-129. <https://doi.org/10.1016/j.quascirev.2006.05.003>.
- Geyman, E.C., Wu, Z., Nadeau, M.D., Edmonson, S., Turner, A., Purkis, S.J., Howes, B., Dyer, B., Ahm, A.S.C., Yao, N. & Deutsch, C.A. 2022. The origin of carbonate mud and implications for global climate. *Proc. Nat. Acad. Sci.*, 119(43): p.e2210617119.
- Gingele, F.X., De Deckker, P. & Hillenbrand, C.D. 2004. Late Quaternary fluctuations of palaeoproductivity in the Murray Canyons area, South Australia. *Paleogeography, Palaeoclimatology, Palaeoecology*, 211(3-4): 235-247.
- Grassle, J.F. & Sanders, H.L. 1973. Life histories and the role of disturbance. *Deep-sea Res.*, 20: 643-659.
- Hahn A., Compton J.S. & Meyer-Jacob C. 2016. Holocene paleo-climatic record from the South African Namaqualand mud belt: A source to sink approach. *Quaternary Int.*, 404: 121-135. <https://doi.org/10.1016/j.quaint.2015.10.017>.
- Hu, B., Yang, Z., Zhao, M., Saito, Y., Fan, D. & Wang, L. 2012. Grain size records reveal variability of the East Asian Winter Monsoon since the Middle Holocene in the Central Yellow Sea mud area, China. *Sci. China Earth Sci.*, 55: 1656-1668.
- Huang, C., Li, M., Liu, Z., Wei, G., Chen, F., Kong, D., Huang, X. & Ye, F. 2020. A high-resolution sediment record of East Asian summer monsoon from the northern South China Sea spanning the past 7500 years. *Holocene*, 30(12): 1669–1680. <https://doi.org/10.1177/0959683620950445>.
- Huang, E., Tian, J., Qiao, P., Wan, S., Xie, X. & Yang, W. 2015. Early interglacial carbonate-dilution events in the South China Sea: Implications for strengthened typhoon activities over subtropical East Asia. *Quaternary Sci. Rev.*, 125: 61-77.
- Isla, E. 2016. Organic carbon and biogenic silica in marine sediments in the vicinities of the Antarctic Peninsula: spatial patterns across a climatic gradient. *Polar Biolog.*, 39(5): 819–828. <https://doi.org/10.1007/s00300-015-1833-6>.
- Jaccard, S.L., Galbraith, E.D., Sigman, D.M. & Haug, G.H. 2010. A pervasive link between Antarctic ice core and subarctic Pacific sediment records over the past 800 kyrs. *Quaternary Sci. Rev.*, 29(1–2): 206–212. <https://doi.org/10.1016/j.quascirev.2009.10.007>.
- Jiwarungrueangkul, T., Liu, Z. & Zhao, Y. 2019. Terrigenous sediment input responding to sea level change and East Asian monsoon evolution since the last deglaciation in the southern South China Sea. *Glob. Planet. Change*, 174: 127–137. <https://doi.org/10.1016/j.gloplacha.2019.01.011>.
- Kamaruzzaman, B.Y., Ong, M.C., Noor Azhar, M.S., Shahbudin, S. & Jalal, K.C.A. 2008. Geochemistry of sediment in the major estuarine mangrove forest of Terengganu region, Malaysia. *Am. J. Applied Sci.*, 5(12): 1707-1712.
- Kok, P.H., Wijeratne, S., Akhir, M.F., Pattiaratchi, C., Chung, J.X., Roseli, N.H. & Daud, N.R., 2022. Modeling approaches in the investigation of upwelling along the east coast of Peninsular Malaysia: Its driven mechanisms. *Reg. Stud. Mar. Sci.*, 55, p.102562.
- Li, D.W., Chang, Y.P., Li, Q., Zheng, L., Ding, X. & Kao, S.J. 2018. Effect of sea-level on organic carbon preservation in the Okinawa Trough over the last 91 kyr. *Mar. Geo.*, 399: 148-157.
- Liu X., Rendle-Buhring R. & Henrich R. 2017. Geochemical composition of Tanzanian shelf sediments indicates Holocene climatic and sea-level changes., *Quaternary Res.*, 87(3): 442–454.
- Liu, S., Zhang, H., Cao, P., Liu, M., Ye, W., Chen, M.T., Li, J., Pan, H.J., Khokiattiwong, S., Kornkanitnan, N. & Shi, X., 2021. Paleoproductivity evolution in the northeastern Indian Ocean since the last glacial maximum: Evidence from biogenic silica variations. *Deep Sea Res. Part I: Oceanographic Res. Papers*, 175: p.103591.
- Liu, X., Zhang, M., Li, A., Dong, J., Zhang, K., Gu, Y., Chang, X., Zhuang, G., Li, Q. & Wang, H. 2022. Sedimentary pyrites and C/S ratios of mud sediments on the East China Sea inner shelf

- indicate late Pleistocene-Holocene environmental evolution. *Mar. Geol.*, 450: p.106854.
- Mann, T., Bender, M., Lorscheid, T., Stocchi, P., Vacchi, M., Switzer, A. D. & Rovere, A. 2019. Holocene sea levels in Southeast Asia, Maldives, India and Sri Lanka: The SEAMIS database. *Quaternary Sci. Rev.*, 219: 112–125. <https://doi.org/10.1016/j.quascirev.2019.07.007>
- Mesa-Fernández, J.M., Martínez-Ruiz, F., Rodrigo-Gámiz, M., Jiménez-Espejo, F.J., García, M. & Sierro, F.J., 2022. Paleocirculation and paleoclimate conditions in the western Mediterranean basins over the last deglaciation: new insights from sediment composition variations. *Glob. Planet. Change*, 209: p.103732.
- Morse, J.W., Arvidson, R.S. & Lüttge, A. 2007. Calcium carbonate formation and dissolution. *Chemical Reviews*, 107(2): 342–381. <https://doi.org/10.1021/cr050358j>.
- Mortlock, R.A. & Froelich, P.N. 1989. A simple method for the rapid determination of biogenic opal in pelagic marine sediments. *Deep Sea Res. Part A, Oceanographic Res. Papers*, 36(9): 1415–1426. [https://doi.org/10.1016/0198-0149\(89\)90092-7](https://doi.org/10.1016/0198-0149(89)90092-7).
- Naim, E., Shaari, H. & Akhir, M.F. 2019. Paleoproductivity Variation in Terengganu Offshore. *Malaysian J. Analytical Sci.* 23(6): 1009–1017.
- Nasir, F., Roslee, A., Zakaria, J., Ariffin, E.H. & Mokhtar, N.A., 2022. Shoreline identification bias: theoretical and measured value for meso-tidal beaches in Kuala Nerus, Terengganu (Malaysia). *J. Mar. Sci. App.*, 21(3): 184-192.
- Ragueneau, O., Tréguer, P., Leynaert, A., Anderson, R.F., Brzezinski, M.A., DeMaster, D.J., Dugdale, R.C., Dymond, J., Fischer, G., François, R., Heinze, C., Maier-Reimer, E., Martin-Jézéquel, V., Nelson, D.M. & Quéguiner, B. 2000. A review of the Si cycle in the modern ocean: Recent progress and missing gaps in the application of biogenic opal as a paleoproductivity proxy. *Global and Planetary Change*, 26(4): 317–365. [https://doi.org/10.1016/S0921-8181\(00\)00052-7](https://doi.org/10.1016/S0921-8181(00)00052-7).
- Shaari, H., Chuan, O.M. & Yunus, K. 2009. Seasonal Distribution of Organic Carbon in the Surface Sediments of the Terengganu Nearshore Coastal Area. *American J. Environ. Sci.*, 5(1): 111–115. <https://doi.org/10.3844/ajessp.2009.111.115>.
- Shapiro, L. & Brannock, W.W. 1962. Rapid Analysis of Silicate, Carbonate and Phosphate Rocks (Issue 1144). U.S. Government Printing Office. <https://books.google.com.my/books?id=SRUPA AAAIAAJ>.
- Sharif, H., Shaari, H., Minhat, F., Nik Shirajuddin, S., Naim, E., Akhi, M. & Sheikh, M. 2024. Ca/Al and Ca/Fe as Indicators of Terrigenous and Marine Origin in East Coast Peninsular Malaysia During Holocene. *Orient. J. Chem.*, 40: p.1261. <https://doi.org/10.13005/ojc/400507>
- Smith, D.E., Harrison, S., Firth, C.R. & Jordan, J.T. 2011. The early Holocene sea level rise. *Quaternary Sci. Reviews*, 30(15–16): 1846–1860. <https://doi.org/10.1016/j.quascirev.2011.04.019>.
- Song, J. 2010. Biogeochemical Processes of the South China Sea. *Advanced Topics in Science and Technology in China*, pp.529–626. Berlin, Heidelberg: Springer Berlin Heidelberg. [https://doi.org/10.1007/978-3-642-04060-3\\_5](https://doi.org/10.1007/978-3-642-04060-3_5)
- Sun, W.P., Hu, C.Y., Han, Z.B., Shen, C., Zhang, W.Y., Zhu, J.H., Yu, P.S., Zhang, H.F. & Pan, J.M. 2020. Variations of diatom opal Ge/Si in Prydz Bay, East Antarctica. *Mar. Chem.*, 227: p.103879.
- Tam, C.Y., Zong, Y., Hassan, K. bin, Ismal, H. bin, Jamil, H. binti, Xiong, H., Wu, P., Sun, Y., Huang, G. & Zheng, Z. 2018. A below-the-present late Holocene relative sea level and the glacial isostatic adjustment during the Holocene in the Malay Peninsula. *Quaternary Sci. Rev.*, 201: 206–222. <https://doi.org/10.1016/j.quascirev.2018.10.009>
- Tribouillard, N., Algeo, T.J., Lyons, T. & Riboulleau, A. 2006. Trace metals as paleoredox and paleoproductivity proxies: An update. *Chem. Geol.*, 232(1–2): 12–32. <https://doi.org/10.1016/j.chemgeo.2006.02.012>.
- Twarog, M.R., Culver, S.J., Mallinson, D.J., Leorri, E., Donovan, B., Harrison, E.I., Hindes, H., Reed, D., Horsman, E., Azhar, N., Shazili, M. & Parham, P.R. 2021. Depositional environments and sequence stratigraphy of post-last glacial maximum incised valley-fill, Malay Basin, northern Sunda Shelf. *Mar. Geol.*, 436: 106457. <https://doi.org/10.1016/j.margeo.2021.106457>.
- Wang, B., Lei, H., Huang, F., Kong, Y., Pan, F., Cheng, W., Chen, Y. & Guo, L. 2020. Effect of Sea-Level Change on Deep-Sea Sedimentary Records in the Northeastern South China Sea over the past 42 kyr. *Geofluids*, 2020(1): p.8814545. <https://doi.org/10.1155/2020/8814545>.

- Xia, J., Han, Y., Tan, J., Abarike, G.A. & Song, Z. 2022. The characteristics of organic carbon in the offshore sediments surrounding the Leizhou Peninsula, China. *Front. Earth Sci.*, 10: p.648337.
- Xu, J., Huang, C. & Huang, X. 2022. Holocene East Asian Summer Monsoon Variation Recorded by Sensitive Grain Size Component from the Pearl River-Derived Mud in the Northern South China Sea. *Lithosphere*, 9: p.6064591. <https://doi.org/10.2113/2022/6064591>
- Xu, Y., Wang, L., Lai, Z., Xu, X., Wang, F., Liu, S., Shi, X., Troa, R.A., Zuraida, R., Triarso, E. & Hendrizan, M. 2019. The biogenic silica variation and paleoproductivity evolution in the eastern Indian Ocean during the past 20 000 a. *Acta Oceanol. Sin.*, 38(1): 78–84. <https://doi.org/10.1007/s13131-019-1372-z>.
- Yang, W., Zheng, H., Xie, X., Zhou, B. & Cheng, X. 2008. East Asian summer monsoon maximum records in northern South China Sea during the early Holocene. *Quaternary Sci.*, 28(3): 425–430.
- Yun, P.S., Ariffin, J., Siang, H.Y. & Tahir, N.M. 2015. Influence of Monsoon on the Distribution of Organic Carbon in Inner Continental. *Sains Malaysiana*, 44(7): 941–945.
- Zhang, L., Wang, R., Chen, M., Liu, J., Zeng, L. & Xiang, R. 2015. Deep-Sea Research II Biogenic silica in surface sediments of the South China Sea: Controlling factors and paleoenvironmental implications. *Deep-Sea Res. Part II*, 122: 142–152. <https://doi.org/10.1016/j.dsr2.2015.11.008>.
- Zhang, Y., Zong, Y., Xiong, H., Li, T., Fu, S., Huang, G. & Zheng, Z. 2021. The middle-to-late Holocene relative sea-level history, highstand and levering effect on the east coast of Malay Peninsula. *Global and Planetary Change*, 196: p.103369. <https://doi.org/10.1016/j.gloplacha.2020.103369>.
- Zhao, X., Dupont, L., Schefuß, E., Bouimetarhan, I. & Wefer, G. 2017. Palynological evidence for Holocene climatic and oceanographic changes off western South Africa. *Quaternary Sci. Rev.*, 165: 88–101.
- Zhou, T., Zhu, Q., Zhu, H., Zhao, Q., Shi, Z., Zhao, S., Zhang, C., Qi, L., Sun, S. & Zhang, Z. 2023. Relative Sea-Level Fluctuations during Rhuddanian–Aeronian Transition and Its Implication for Shale Gas Sweet Spot Forming: A Case Study of Luzhou Area in the Southern Sichuan Basin, SW China. *J. Mar. Sci. Eng.*, 11: p.1788. <https://doi.org/10.3390/jmse11091788>.